Local order in amorphous $Ge_2Sb_2Te_5$ and $GeSb_2Te_4$

P. Jóvári,[1] I. Kaban,[2] J. Steiner,[3] B. Beuneu,[4] A. Schöps,[5] and M. A. Webb[5]
[1]*Research Institute for Solid State Physics and Optics, Hungarian Academy of Sciences, P.O. Box 49, Budapest H-1525, Hungary*
[2]*Institute of Physics, Chemnitz University of Technology, D-09107 Chemnitz, Germany*
[3]*I. Physikalisches Institut, RWTH Aachen, Physik neuer Materialien, 52056 Aachen, Germany*
[4]*Laboratoire Léon Brillouin, CEA/Saclay, 91191 Gif-Sur-Yvette Cedex, France*
[5]*HASYLAB am Deutschen Elektronen Synchrotron, DESY, Notkestrasse 85, D-22603 Hamburg, Germany*
(Received 25 September 2007; revised manuscript received 30 October 2007; published 2 January 2008)

The structure of amorphous $Ge_2Sb_2Te_5$ and $GeSb_2Te_4$ phase-change alloys was investigated by high energy x-ray diffraction, extended x-ray-absorption fine structure, and neutron diffraction. The reverse Monte Carlo simulation technique was used to generate large scale atomic models compatible with all experimental data sets. Simulations revealed that Ge-Ge bonding is present already in $GeSb_2Te_4$. Ge-Sb bonding was also found to be significant for both compositions. Within experimental uncertainties, all atomic species satisfy formal valence requirements: Ge is fourfold coordinated, Sb has three neighbors, and Te is mostly twofold coordinated. The environment of Ge atoms was investigated in detail. The predominance of $GeTe_4$ or Te_3Ge-$GeTe_3$ units in these compositions can be excluded. Instead, these alloys are characterized by a variety of local motifs.

DOI: 10.1103/PhysRevB.77.035202 PACS number(s): 61.43.Dq, 61.05.cj, 61.05.cp, 61.05.fm

I. INTRODUCTION

It was more than 35 years ago when Feinleib *et al.*[1] reported on a reversible laser induced amorphous-to-crystalline transition and a pronounced contrast of optical properties between amorphous and crystalline states in the $Te_{81}Ge_{15}Sb_2S_2$ film. The practical importance of this order-disorder phase-change memory effect was recognized immediately and intense investigations started. Later, it was suggested[2] that due to their favorable properties (short crystallization time, excellent reversibility between the amorphous and crystalline states, and high thermal stability), compositions along the $GeTe$-Sb_2Te_3 tie line (e.g., $Ge_2Sb_2Te_5$ and $GeSb_2Te_4$) are the best recording materials for rewritable optical memories. The phase-change technology has progressed continuously. According to a recent publication, the highest—noncommercial—storage capacity realized with a $Ge_2Sb_2Te_5$ film is on the order of 60 GB/cm^2 now.[3] This value is about 10^4 higher than the performance of the early compact disk technology.

Comparison of recent experimental studies reveals that despite its technological importance, the structure of $Ge_2Sb_2Te_5$ is still debated. The "umbrella flip" mechanism of order-disorder transition of $Ge_2Sb_2Te_5$ was proposed by Kolobov *et al.*[4] According to this model, amorphization is accompanied by a jump of a Ge atom from the octahedral site occupied in the crystal to a tetrahedral position surrounded by four Te atoms. Therefore, each Ge is coordinated by four Te atoms, and Ge-Ge and Sb-Ge bonds cannot be found (or, at least, are not significant) in the amorphous structure. From the similarity of Sb *K*-edge x-ray appearance near edge structure spectra in the two phases, it was inferred that the arrangement of atoms around Sb remains practically unchanged during amorphization, which means that Sb atoms are bound only to Te in both phases. Thus, according to Ref. 4, there are only Ge-Te and Sb-Te bonds in amorphous $Ge_2Sb_2Te_5$.

Baker *et al.* combined bond constraint theory and coordination numbers extracted from extended x-ray-absorption fine structure (EXAFS) spectra of amorphous $Ge_2Sb_2Te_5$.[5–7] They concluded that 17% of Te atoms are overcoordinated and Ge atoms are involved in Te_3Ge-$GeTe_3$ structural units. In contrast to the umbrella flip mechanism, this model is based on the preferential formation of Ge-Ge bonds.

More recently, Kohara *et al.* carried out an x-ray diffraction study on the structure of amorphous, liquid, and crystalline $Ge_2Sb_2Te_5$.[8] The experimental structure factor was fitted by the reverse Monte Carlo (RMC) simulation technique[9–11] by assuming that there are no Ge-Ge, Ge-Sb, and Sb-Sb bonds in amorphous $Ge_2Sb_2Te_5$. The analysis of the obtained particle configuration showed that similar to the crystalline state, ring size distribution is dominated by four- and six-membered rings, which can be the key for fast crystallization. Simulations gave the same results regardless of the starting configuration (crystalline or random hard sphere). It was also shown that even if Ge-Ge, Ge-Sb, and Sb-Sb bonds were allowed, the ring size distribution was dominated by even-membered rings. Though this model is simple and straightforward, experimental observations do not lend sufficient support to it. The main problems are that Sb and Te are practically indistinguishable by x-ray diffraction and the weights of Ge-Ge and Ge-Sb correlations in the experimental data are too low (~2% and ~7%, respectively), thus—regardless of the method used for data evaluation or modeling—a good fit of a single x-ray measurement does not necessarily mean that these bonds are really missing from amorphous $Ge_2Sb_2Te_5$.

Comparison of the above models illustrates that the structure of amorphous Ge-Sb-Te alloys is still not understood. In the case of insufficient experimental information, the uncertainty of data interpretation can prevent us from setting up realistic structural models. It is well illustrated by the coordination numbers, which are either not reported[4] or their uncertainty is too large—25% for Te,[5] the major component of $Ge_2Sb_2Te_5$. The error of structural parameters can be decreased only by combining the information offered by different techniques. The uncertainty of x-ray- or neutron-weighted total coordination numbers is usually around 5%–

10%. Due to the higher neutron scattering length of Ge, the weight of Ge-Ge and Ge-Sb partial structure factors is significantly higher in the neutron diffraction measurement (8.4% and 11.4%, respectively). Thus, a model structure accounting for both neutron and x-ray structure factors could already give a more accurate determination of Ge-related structural parameters. However, an additional difficulty of Ge-Sb-Te alloys is the similarity of Sb and Te neutron scattering lengths (5.58 and 5.80 fm, respectively), which means that these atoms are indistinguishable by neutrons as well. They are also very similar as photoelectron backscatterers, thus a Ge *K*-edge EXAFS measurement alone cannot distinguish between Ge-Te and Ge-Sb pairs. This degeneracy can be resolved by Sb and Te *K*-edge data. (As Ge and Te possess rather different backscattering powers, Sb-Ge and Sb-Te/Sb correlations can be resolved by an Sb *K*-edge measurement.)

The structure of sputtered amorphous $Ge_2Sb_2Te_5$ was investigated recently by modeling simultaneously x-ray diffraction, neutron diffraction, and EXAFS measurements.[12] The five data sets were fitted simultaneously by the reverse Monte Carlo simulation technique. RMC is an iterative procedure that seeks three-dimensional structures compatible with measured data through random atomic moves. Moves are always accepted if they improve the agreement between experimental data sets and model curves calculated from atomic coordinates. To prevent simulation from being trapped into local minima, a fraction of moves leading to a weaker fit is also accepted. Interatomic potentials are not needed to run RMC, but results strongly rely on the density of the system and minimum interatomic distances. As it is emphasized in Ref. 13, the use of these parameters and the simultaneous fit of several data sets act as powerful constraints in modeling disordered systems. It was found that Ge-Ge and Ge-Sb bondings are significant in amorphous $Ge_2Sb_2Te_5$, which clearly indicates that the models proposed in Refs. 4–8 can be compatible with the limited experimental information they are based on, but are certainly not consistent with all of the five measurements modeled in Ref. 12.

II. RESULTS AND DISCUSSION

To gain a more profound knowledge on the structure of amorphous Ge-Sb-Te alloys, we extended our investigations in two directions. (i) we carried out diffraction and EXAFS measurements on $GeSb_2Te_4$ as well. Due to its simpler stoichiometry, this composition is also heavily investigated, especially by electronic structure calculation methods.[14] Comparison of two compositions lying along the GeTe-Sb_2Te_3 tie line will help us in drawing more general conclusions. (ii) To reveal which local atomic environments contribute to the structure of $GeSb_2Te_4$ and $Ge_2Sb_2Te_5$, we also performed simulations using a different RMC code.[15] This version allows the use of sophisticated constraints (e.g., the total number of neighbors of an atom of a given type), thus it is an ideal tool for modeling multicomponent covalent glasses. We refer to Ref. 12 for details of experiments. For simultaneous modeling of several data sets, see Ref. 16.

To check the possible differences between the structure of amorphous $Ge_2Sb_2Te_5$ and $GeSb_2Te_4$, we carried out an unconstrained simulation run on $GeSb_2Te_4$ first. The simulation box contained 36 400 atoms with the proper stoichiometry. Different cutoff distances were used to test whether Ge-Ge, Ge-Sb, Sb-Sb, and Te-Te bonds exist in this alloy. It was found that (similar to the case of $Ge_2Sb_2Te_5$) Sb-Sb and Te-Te bondings are not significant in $GeSb_2Te_4$, while Ge-Ge and Ge-Sb bonds should be allowed to get a good fit. The effect of Ge-Sb bonding on the fit of Sb *K*-edge EXAFS data is shown in Fig. 1. The change in the fit quality shows that Sb-Ge bonding is significant in $GeSb_2Te_4$. It should be mentioned that the mean Ge-Sb interatomic distance (2.69 ± 0.02 Å) agrees very well with the sum of covalent radii (2.68 Å). Other fits are presented in Fig. 2. In these unconstrained runs, the average number of neighbors of Ge, Sb, and Te was 4.01, 3.40, and 2.06, respectively. These values strongly suggest that similar to $Ge_2Sb_2Te_5$ amorphous $GeSb_2Te_4$ is also a covalent network in which all (or, at least, the majority of) atoms satisfy the "$8-N$" rule.[17] It should be emphasized that the above values have been obtained without constraining the average number of neighbors. Conformity with the $8-N$ rule is, thus, not a consequence of some presumptions, but follows directly from the experimental data modeled in this study.

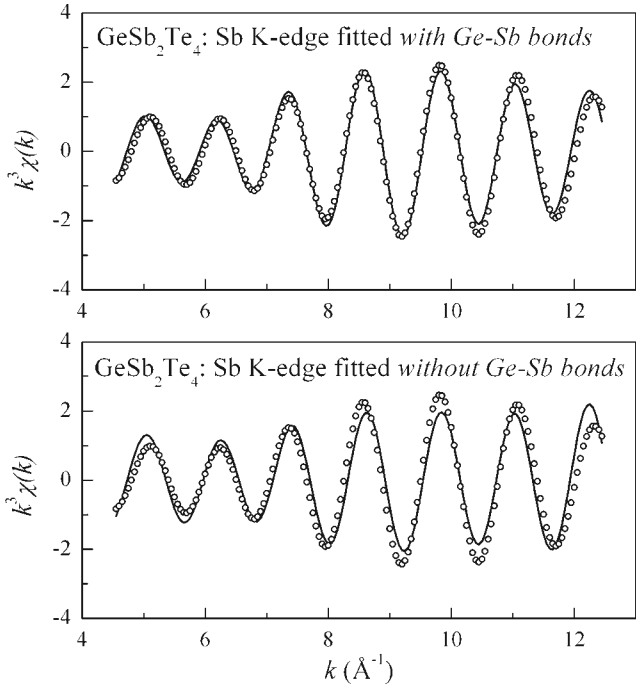

FIG. 1. Sb *K*-edge EXAFS spectrum for sputtered amorphous $GeSb_2Te_4$. Circles, measured; lines, obtained by simultaneous RMC simulation (unconstrained case) of the experimental XRD, ND, and EXAFS data with and without Ge-Sb bonds.

To learn more about the atomic level structure, we carried out constrained simulations, in which *each* Ge, Sb, and Te atom was forced to have four, three, and two neighbors, respectively, but the type of neighbors was not constrained. In the final configurations selected for detailed analysis, 90%–95% of the atoms satisfied the above constraints. Even in this case excellent fits could be achieved (Fig. 3 for $Ge_2Sb_2Te_5$). Coordination numbers N_{ij} and mean interatomic distances r_{ij}

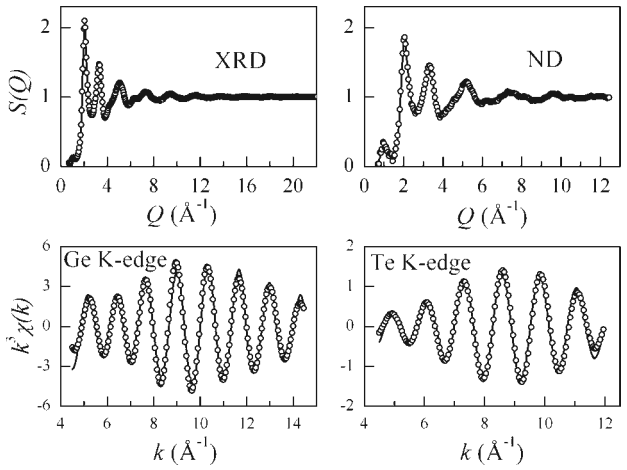

FIG. 2. XRD and ND structure factors, and EXAFS spectra for as-sputtered amorphous $GeSb_2Te_4$. Circles, measured; lines, obtained by simultaneous RMC simulation (unconstrained case) of the experimental XRD, ND, and EXAFS data. The fit of Sb *K*-edge is shown in Fig. 1.

for both as-sputtered amorphous $Ge_2Sb_2Te_5$ and $GeSb_2Te_4$ are listed in Table I, while partial pair correlation functions are shown in Fig. 4. Due to EXAFS measurements, the uncertainty of bond lengths is about 0.02 Å. As the error of neutron- and x-ray-weighted coordination numbers is about 5%–10%, the uncertainty of coordination numbers is smaller than that achievable by EXAFS. The error of Te, Ge, and Sb

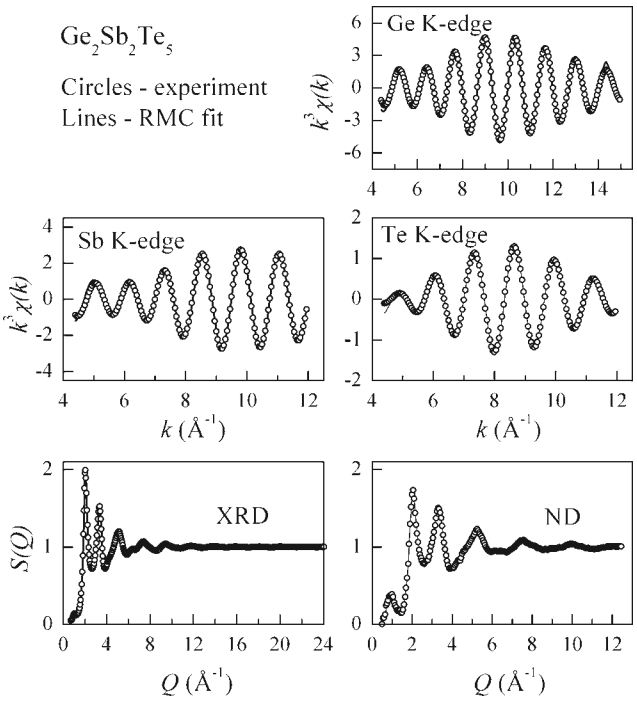

FIG. 3. XRD and ND structure factors, and EXAFS spectra for as-sputtered amorphous $Ge_2Sb_2Te_5$. Circles, measured; lines, obtained by simultaneous RMC simulation of the experimental XRD, ND, and EXAFS data. Ge, Sb, and Te atoms were forced to have four, three, and two neighbors, respectively, but the type of neighbors was not constrained.

coordination numbers is around 0.2–0.4 in the unconstrained runs. In the constrained runs, these coordination numbers are very close to the target values. The unchanged quality of the fits corroborates the validity of the $8-N$ model. Coordination numbers not listed in Table I can be obtained by the following formula: $N_{ij}=(c_j/c_i)N_{ji}$, where c_i and c_j denote the concentration of species i and j. Some small spikes can be observed at about 3–3.2 Å on some of the partial pair correlation functions. The position of these features varied with the upper limit of nearest neighbor distances used in the constraints. Regardless of the method of analysis, the definition of the first coordination sphere is always somewhat arbitrary if the first minimum value of the partial pair correlation functions is not zero. The uncertainty of coordination numbers caused by the spikes is small (~5%) and does not affect the conclusions of this study. The similarity of the corresponding partial pair correlation functions of $Ge_2Sb_2Te_5$ and $GeSb_2Te_4$ is remarkable. Peak positions agree even in the case of $g_{GeGe}(r)$ and $g_{GeSb}(r)$. Taking into account the low concentration of these atoms, differences in peak shape are not significant.

It can be observed in both alloys that N_{TeSb}/N_{TeGe} is very close to c_{Sb}/c_{Ge}, the ratio of Sb and Ge concentrations. On the other hand, our results show the presence of marked bonding preferences around Sb and Ge. For example, in $Ge_2Sb_2Te_5$ $N_{GeTe}/N_{GeSb}\approx 4$, while c_{Te}/c_{Sb} is only 2.5. Similarly, $N_{SbTe}/N_{SbGe}\approx 4.1$, but c_{Te}/c_{Ge} is only 2.5. Te-Ge and Te-Sb bonds are, thus, clearly preferred to Ge-Sb ones. Ge-Ge partial pair correlation functions exhibit a very pronounced first peak at 2.48 Å. $N_{GeGe}/N_{Ge\text{-}X}$ (where $N_{Ge\text{-}X}$ is the total number of neighbors around Ge) is in both cases close to c_{Ge}. From this it can be anticipated that Ge-Ge bonding is even more significant at higher Ge concentrations.

At this point, it may be interesting to compare the bond lengths and coordination numbers obtained in the present work with results of some recent EXAFS studies on $Ge_2Sb_2Te_5$. It can be observed that the agreement between Ge-Te and Sb-Te mean interatomic distances is usually satisfactory. Kolobov *et al.* obtained 2.61 Å for the Ge-Te mean interatomic distance,[4] while Baker *et al.* got 2.63±0.01 Å.[5–7] Both values are close to the Ge-Te distance obtained in the present work (2.60 Å). Sb-Te bond lengths (2.85 Å in Ref. 4 and 2.83 Å in Refs. 5–7) also agree within experimental errors. In contrast to the similarity of Ge-Te and Sb-Te bond lengths, the uncertainty of type and number of nearest neighbors is much larger. No coordination numbers were reported at all in Ref. 4, while Ge-Ge bonding was reported only in Refs. 5–7. Both the bond length (2.47 Å) and the average coordination number (0.6±0.2) agree reasonably with the values of the present study (2.48 Å and 0.77, respectively). The environment of Sb atoms is perhaps the source of greatest uncertainties. Three different interpretations of Sb *K*-edge data were reported by Baker *et al.* in Refs. 5–7. Besides Sb-Te bonding, they considered Sb-Sb pairs at a distance as low as 2.44 Å (Ref. 6) or Sb-Te^+ contact at a separation of 2.51 Å.[7] We believe that the introduction of Sb-Ge pairs is simple, plausible, and is supported by our results (see Fig. 1).

In a very recent study, hard x-ray photoemission spectroscopy was used to investigate the electronic structure of amor-

TABLE I. Bond lengths r_{ij} (Å), coordination numbers N_{ij}, and the total number of neighbors of a given atomic species (Te-*X* etc.) in as-sputtered amorphous $Ge_2Sb_2Te_5$ and $GeSb_2Te_4$ obtained from models generated by RMC. Ge, Sb, and Te atoms were forced to have four, three, and two neighbors, respectively, but the type of neighbors was not constrained. The bond length accuracy is ±0.02 Å.

Alloy	Parameter	Te-Sb	Te-Ge	Sb-Ge	Ge-Ge	Te-*X*	Sb-*X*	Ge-*X*
$Ge_2Sb_2Te_5$	r_{ij}	2.82	2.60	2.69	2.48			
	N_{ij}	1.01	0.98	0.60	0.79	1.99	3.12	3.85
$GeSb_2Te_4$	r_{ij}	2.83	2.61	2.69	2.48			
	N_{ij}	1.29	0.69	0.33	0.49	1.98	2.91	3.91

phous and crystalline $(GeTe)_{1-x}$-$(Sb_2Te_3)_x$ alloys.[18] The authors concluded that the valence band structure does not change drastically between the crystalline and amorphous phases. They also found that due to the high concentration of vacancies, crystalline and amorphous phases possess the same "local disorder." These—together with the results of Ref. 8 (Te-centered bond angles are distributed around 90° and Sb/Te has about three neighbors)—led them to the hypothesis that the amorphous-crystalline phase change is essentially a transition between threefold and sixfold coordinated structures. This hypothesis contradicts not only the findings of the present study, but also EXAFS works on $Ge_2Sb_2Te_5$ (Ref. 4) and GeTe,[19] which clearly demonstrate that amorphous and crystalline Ge-Sb-Te alloys possess different local orders.

The structure of amorphous $Ge_2Sb_2Te_5$ was investigated recently by a reverse Monte Carlo simulation study.[20] Some of its results (e.g., the existence of Sb-Ge bonds) agree with the finding of the present work. Nevertheless, the agreement between experimental results and model curves is worse than in the present case, and the first peaks of $g_{GeTe}(r)$, $g_{SbTe}(r)$, and $g_{GeSb}(r)$ are not separated (see Fig. 6 of Ref. 20), which suggests that the experimental evidence [three EXAFS data sets and an x-ray diffraction (XRD) structure factor measured up to 8 $Å^{-1}$] modeled in Ref. 20 is not sufficient to resolve the main structural features of amorphous $Ge_2Sb_2Te_5$.

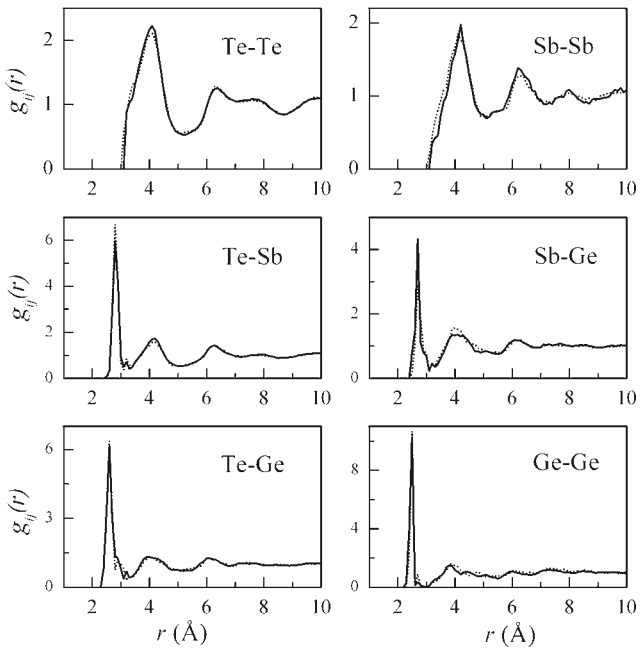

FIG. 4. RMC simulated partial pair correlation functions for as-sputtered amorphous $Ge_2Sb_2Te_5$ (solid lines) and $GeSb_2Te_4$ (dotted lines). Ge, Sb, and Te atoms were forced to have four, three, and two neighbors, respectively, but the type of neighbors was not constrained.

Our results suggest that the similarity between crystalline and amorphous phases exists only in a very special sense: Te-Te (and Sb-Sb) bonds missing from the crystalline state are not significant in the amorphous phase either. Taking into account the high concentration of Te, this is a strong restriction on possible amorphous structures. The other factor determining the structure of amorphous Ge-Sb-Te alloys is that atoms tend to satisfy formal valence requirements (four, three, and two neighbors for Ge, Sb, and Te, respectively), which could be simultaneously satisfied only if Ge-Ge and Ge-Sb bonds are allowed.

It is suggested[8] that bond angle distributions (BAD's) centered on Ge, Sb, and Te are similar in amorphous $Ge_2Sb_2Te_5$ and have their peaks at about 90°. The comparison of Te-Ge-Te and Te-Sb-Te BAD's calculated from the configurations obtained by the simultaneous fit of five data sets reveals the presence of marked differences (Fig. 5). The main peak of Te-Sb-Te BAD is at about 90°–95°. In the case of Te-Sb-Te, there is a minor peak close to 180° showing that some Sb atoms and two of their three neighbors can be found in a linear arrangement, which also means that these Sb atoms and their neighboring Te atoms are in the same plane. The origin of the peak close to 180° was investigated in detail for amorphous $Ge_2Sb_2Te_5$ by carrying out a simulation in which no experimental data sets were fitted but the coordination constraints were applied. The Te-Sb-Te BAD calculated from the resulting configuration is also shown in Fig. 5. This curve is rather structureless apart from a "contact peak" at about 75°–80°, corresponding to the closest approach of two Te atoms bound to the same Sb, which suggests that the shape of the Te-Sb-Te BAD (including the peak close to 180° and the valley between 120° and 150°) is determined by the data fitted.

Figure 6 shows the Te-Ge-Te BAD's of amorphous $Ge_2Sb_2Te_5$ and $Ge_{15}Te_{85}$.[21] In the case of the binary alloy, the peak is at about 107°, which is very close to the tetrahedral angle (109.47°). Due to the asymmetry of $g_{GeTe}(r)$, the

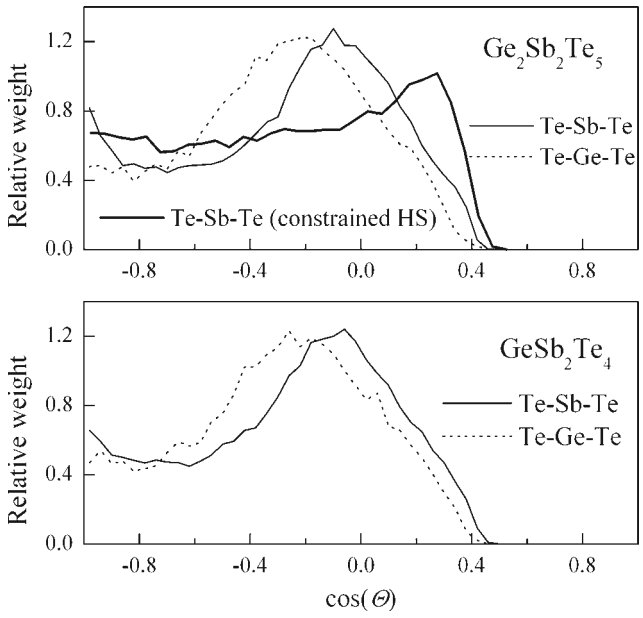

FIG. 5. Comparison of Te-Sb-Te and Te-Ge-Te bond angle distributions for amorphous $Ge_2Sb_2Te_5$ and $GeSb_2Te_4$ (see text for details).

Te-Ge-Te BAD of amorphous $Ge_2Sb_2Te_5$ is somewhat sensitive to the cutoff distance used for bond angle calculations. If Ge-Te pairs are counted up to 3.1 Å, the minimum of $g_{GeTe}(r)$ then is the peak at about 105°. If the maximum Ge-Te distance is decreased to 2.9 Å (the value used for $Ge_{15}Te_{85}$), then the peak shifts toward higher angles. Nevertheless, this effect is small and our results clearly show the differences between Te-Ge-Te and Te-Sb-Te bond angle distributions. Even though Ge is not tetrahedrally coordinated in crystalline GeTe or $Ge_2Sb_2Te_5$, the Te-Ge-Te bond angle distribution (and Ge coordination numbers) suggests that it is in a dominantly tetrahedral environment in amorphous $Ge_2Sb_2Te_5$.

As current models of Ge-Sb-Te phase-change materials concentrate mostly on the environment of Ge atoms (either by supposing that each Ge is involved in Te_3Ge-$GeTe_3$ units[5–7] or by assuming that crystallization is accompanied by a jump of Ge from $GeTe_4$ units to octahedral positions[4]), a more profound analysis of Ge coordination environments was carried out. A detailed statistics of neighbor distribution in GeX_4 (X=Ge, Sb, and Te) tetrahedra is shown in Fig. 7. In the case of $Ge_2Sb_2Te_5$, the most dominant contributions are from $GeGeTe_3$, $GeSbTe_3$, and $GeGeSbTe_2$, giving roughly 55% of GeX_4 tetrahedra. These results suggest the occurrence of short Ge chains in $Ge_2Sb_2Te_5$. The weight of $GeTe_4$ is about 15%. In line with its lower Ge content, $GeTe_4$, $GeSbTe_3$, and $GeGeTe_3$ are the most frequent environments of Ge in $GeSb_2Te_4$, and the weight of species with two or more Ge atoms is significantly lower than in $Ge_2Sb_2Te_5$. Our results show that Ge atoms are mostly tetrahedrally coordinated in amorphous $Ge_2Sb_2Te_5$ and $GeSb_2Te_4$. On the other hand, the predominance of certain local motifs suggested in recent studies—e.g., $GeTe_4$ (Ref. 4) or Te_3Ge-$GeTe_3$ (Refs. 5–7)—is not verified.

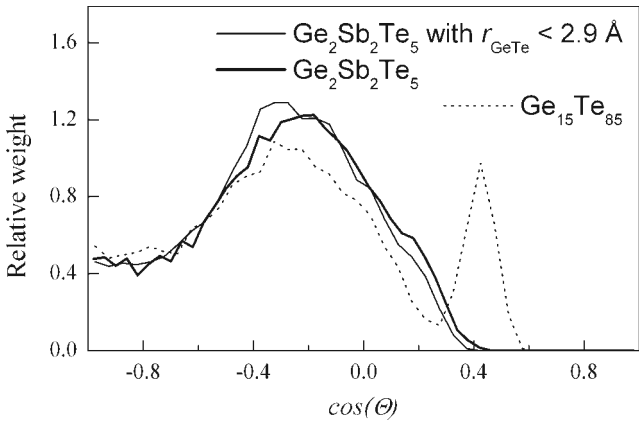

FIG. 6. Comparison of Te-Ge-Te bond angle distributions for amorphous $Ge_2Sb_2Te_5$ and $Ge_{15}Te_{85}$ (Ref. 21) (see text for details).

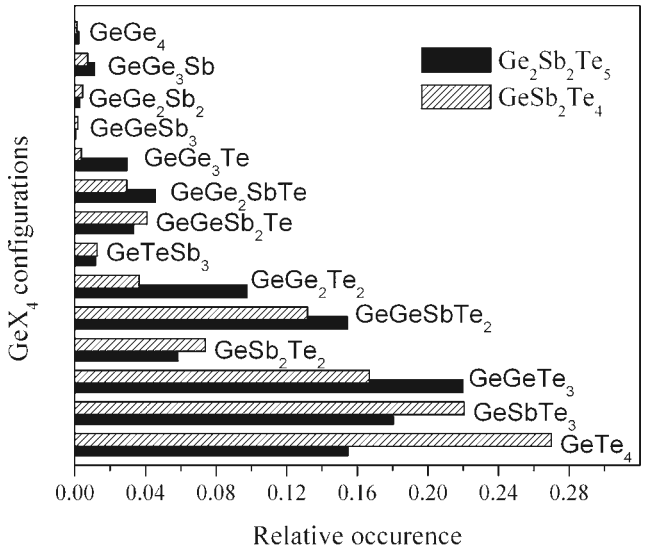

FIG. 7. Statistics of GeX_4 coordination environments in amorphous $Ge_2Sb_2Te_5$ and $GeSb_2Te_4$ obtained from models generated by constrained RMC simulations.

III. CONCLUSIONS

To summarize, in this paper the results of a detailed experimental structural study of amorphous $Ge_2Sb_2Te_5$ and $GeSb_2Te_4$ are presented. Both alloys were investigated by XRD, neutron diffraction (ND), and Ge, Sb, and Te K-edge EXAFS spectroscopy. Data sets were modeled simultaneously by the RMC simulation method. The usage of this technique ensures the consistency of all fits with the *same* model structure. This way the uncertainty of interpretation found to be significant in previous studies could be minimized. The main results of this study are the following:

(1) The simultaneous fitting of the five data sets revealed that—similar to $Ge_2Sb_2Te_5$—Ge-Sb and Ge-Ge bondings are significant in $GeSb_2Te_4$, while Te-Te and Sb-Sb bondings cannot be detected.

(2) *Average* coordination numbers obtained by the above unconstrained reverse Monte Carlo fit revealed that $GeSb_2Te_4$ also satisfies the $8-N$ rule.

(3) By using coordination constraints, configurations were generated, in which the majority of atoms satisfy the $8-N$ rule (90%–95% of Ge, Sb, and Te neighbors have four, three, and two neighbors, respectively). It could be done without any deterioration of the quality of fit, which is a further argument for the validity of the $8-N$ rule.

(4) The statistics of GeX_4 coordination environments was investigated in detail. Our results suggest that the dominance of one or two building blocks or basic motifs can be ruled out in the alloys investigated. Nevertheless, the structure of amorphous $Ge_2Sb_2Te_5$ and $GeSb_2Te_4$ cannot be regarded as a random network. Rather, it is determined by two conflicting conditions: (i) all (or, at least, the vast majority of) atoms tend to satisfy the $8-N$ rule, and (ii) the bonds missing in the crystalline state are more likely to be avoided. The structure of these alloys can be considered as a compromise between the above two conditions: Sb-Sb and Te-Te bondings are not significant (the latter is a very strong constraint at 56%–57% Te content), but the $8-N$ rule can be satisfied only by the formation of Ge-Ge and Ge-Sb bonds, which cannot be found in the crystalline state.

A brief and pictorial structural model of amorphous Ge-Sb-Te alloys is not given here. The gist of this paper is exactly that no such model exists. Our results also suggest that a realistic description of fast switching should rely on the structure and physical properties of all states (crystalline, liquid, and amorphous) involved in phase change.

ACKNOWLEDGMENTS

The x-ray diffraction and EXAFS experiments were supported by Deutsches Elektronen-Synchrotron, DESY. The neutron diffraction measurement at Saclay (France) was supported by the European Commission under the 6th Framework Programme through the Key Action: Strengthening the European Research Area, Research Infrastructures, Contract No. HII3-CT-2003-505925. P.J. was supported by the OTKA (Hungarian Basic Research Found) Grant No. T048580.

[1] J. Feinleib, J. de Neufville, S. C. Moss, and S. R. Ovshinsky, Appl. Phys. Lett. **18**, 254 (1971).
[2] N. Yamada and T. Matsunaga, J. Appl. Phys. **88**, 7020 (2000).
[3] H. F. Hamann, M. O'Boyle, Y. C. Martin, M. Rooks, and H. K. Wickramasinghe, Nat. Mater. **5**, 383 (2006).
[4] A. V. Kolobov, P. Fons, A. I. Frenkel, A. L. Ankudinov, J. Tominaga, and T. Uruga, Nat. Mater. **3**, 703 (2004).
[5] D. A. Baker, M. A. Paesler, G. Lucovsky, S. C. Agarwal, and P. C. Taylor, Phys. Rev. Lett. **96**, 255501 (2006).
[6] D. A. Baker, M. A. Paesler, G. Lucovsky, S. C. Agarwal, and P. C. Taylor, J. Non-Cryst. Solids **352**, 1621 (2006).
[7] M. A. Paesler, D. A. Baker, G. Lucovsky, A. E. Edwards, and P. C. Taylor, J. Optoelectron. Adv. Mater. **8**, 2039 (2006).
[8] S. Kohara, K. Kato, S. Kimura, H. Tanaka, T. Usuki, K. Suzuya, H. Tanaka, Y. Morimoto, T. Matsunaga, N. Yamada, Y. Tanaka, H. Suematsu, and M. Takata, Appl. Phys. Lett. **89**, 201910 (2006).
[9] R. L. McGreevy and L. Pusztai, Mol. Simul. **1**, 359 (1988).
[10] R. L. McGreevy, J. Phys.: Condens. Matter **13**, 877 (2001).
[11] G. Evrard and L. Pusztai, J. Phys.: Condens. Matter **17**, S1 (2005).
[12] P. Jóvári, I. Kaban, J. Steiner, B. Beuneu, A. Schöps, and A. Webb, J. Phys.: Condens. Matter **19**, 335212 (2007).
[13] S. J. Gurman, J. Synchrotron Radiat. **2**, 56 (1995).
[14] M. Wuttig, D. Lüsebrink, D. Wamwangi, W. Welnic, M. Gillessen, and R. Dronkowski, Nat. Mater. **6**, 122 (2007).
[15] O. Gereben, P. Jóvári, L. Temleitner, and L. Pusztai, J. Optoelectron. Adv. Mater. **9**, 3021 (2007); code and executables are available at http://www.szfki.hu/~nphys/rmc++/opening.html
[16] I. Kaban, P. Jóvári, W. Hoyer, and E. Welter, J. Non-Cryst. Solids **353**, 2474 (2007).
[17] N. Mott, Adv. Phys. **16**, 49 (1967).
[18] J.-J. Kim, K. Kobayashi, E. Ikenaga, M. Kobata, S. Ueda, T. Matsunaga, K. Kifune, R. Kojima, and N. Yamada, Phys. Rev. B **76**, 115124 (2007).
[19] A. V. Kolobov, P. Fons, J. Tominaga, A. L. Ankudinov, S. N. Yannopoulos, and K. S. Andrikopoulos, J. Phys.: Condens. Matter **16**, S5103 (2006).
[20] T. Arai, M. Sato, and N. Umesaki, J. Phys.: Condens. Matter **19**, 335213 (2007).
[21] P. Jóvári, I. Kaban, W. Hoyer, R. G. Delaplane, and A. Wannberg, J. Phys.: Condens. Matter **17**, 1529 (2005).